

**AN IMPROVED BLIND SELECTED MAPPING WITH DECODING  
COMPLEXITY REDUCTION FOR ORTHOGONAL FREQUENCY  
DIVISION MULTIPLEXING SYSTEM**

**by**

**ADNAN HAIDER YUSEF SA'D**

**Thesis submitted in fulfilment of the  
requirements for the degree of  
Doctor of Philosophy**

**May 2019**

## ACKNOWLEDGEMENT

Alhamdulillah, First of all, All praise and thanks are due to Almighty Allah, the one who is most deserving of thanks and praise for all great favours and blessings he has bestowed upon us. Next, I would like to express my thanks to my supervisor Dr. Aeizaal Azman bin Abd Wahab for his support and guidance all the way during this research. His advanced level of support helped me to complete this research.

Beside my supervisor, I would like to sincerely thank Dr. Nor Muzlifah Mahyuddin for her support and her influence on my research. I would like to thank USM as well for the GA opportunity.

I wish also to express my deepest gratitude, thanks, and indebtedness to my beloved parents: Haider Yusef and Huda Abdullah, for their overwhelming love, supports, and prayers that led me to this great point in my life. My profound gratitude, love, and thanks also go to my dear wife Amaal who kept supporting me enormously throughout my PhD. Also, I would like to express my love and thanks to my wonderful children: Motasim and Raghad, for always making me smile.

Finally, the last but not least, I would like to thank my siblings, my whole family and all friends who kept encouraging me and pushing me forward to pursue and finish my PhD study.

# TABLE OF CONTENTS

	<b>Page</b>
<b>ACKNOWLEDGEMENT</b>	<b>ii</b>
<b>TABLE OF CONTENTS</b>	<b>iii</b>
<b>LIST OF TABLES</b>	<b>vii</b>
<b>LIST OF FIGURES</b>	<b>x</b>
<b>LIST OF ABBREVIATIONS</b>	<b>xvii</b>
<b>ABSTRAK</b>	<b>xix</b>
<b>ABSTRACT</b>	<b>xxi</b>
<b>CHAPTER ONE: INTRODUCTION</b>	
1.1 Background	1
1.2 Problem Statement	3
1.3 Objectives	7
1.4 Project Scope	7
1.5 Thesis Outlines	9
<b>CHAPTER TWO: LITERATURE REVIEW</b>	
2.1 Introduction	11
2.2 OFDM	12
2.3 Peak-to-Average Power Ratio (PAPR)	16
2.4 PAPR Reduction	19
2.5 Preserving Data Rate (Blind SLM)	27
2.5.1 Pilot-based Blind SLM	28
2.5.2 Data-based Blind SLM	37
2.5.2(a) Energy disparity based BSLM	39
2.5.2(b) Phase-based blind SLM	45

2.6	Conventional BSLM Scheme	59
2.7	Summary	62
<b>CHAPTER THREE: METHODOLOGY</b>		
3.1	Introduction	64
3.2	Implementation Flow Chart	65
3.3	BSLM transmitter	67
3.4	BSLM receiver	68
3.5	Performance Analysis Methods	71
3.5.1	Channels:	72
3.5.1(a)	AWGN Channel:	72
3.5.1(b)	Rayleigh Channel:	74
3.5.2	ANOVA	75
3.6	Implementation parameters	77
3.7	Summary	78
<b>CHAPTER FOUR: RECEIVER DESIGN</b>		
4.1	Introduction	79
4.2	ML decoder using Prior Knowledge (MLPK)	80
4.2.1	MLPK for PSK	82
4.2.2	MLPK for QAM	84
4.3	Complexity Reduction ( <b>q</b> Parameter)	87
4.3.1	Complexity Reduction - Symmetry Property	87
4.3.1(a)	MLPK with Symmetry Property	92
4.3.2	PSK Property-based Decoder - Phase Property	93
4.3.2(a)	PSK Property-based MLPK decoder	97
4.3.3	QAM Property-based Decoder - Rectangular Shape Property	101

4.3.3(a)	QAM Property-based MLPK decoder	105
4.4	Complexity Reduction ( <b>N</b> Parameter)	108
4.4.1	SNR-dependent Method	108
4.4.2	Complexity Reduction - SNR-independent	111
4.5	Complexity Reduction ( <b>U</b> parameter)	113
4.6	Decoding In Two Lattices	114
4.6.1	MLPK with Two Lattices Decoding Capability	115
4.6.1(a)	PSK	115
4.6.1(b)	QAM	115
4.6.2	Non-MLPK with Two Lattices Decoding Capability	118
4.6.2(a)	PSK	119
4.6.2(b)	QAM	120
4.7	Optimizing Complex Multiplications	123
4.8	BSLM Receiver Designs	124
4.9	Retrieving Original Data – (Descrambling & Decoding)	125
4.10	Summary	130
<b>CHAPTER FIVE: RESULTS AND DISCUSSION</b>		
5.1	Introduction	132
5.2	Performance of BSLM (MLPK)	132
5.3	Performance of BSLM ( <b>q</b> Parameter)	134
5.3.1	Decoding In Own Lattice	141
5.4	Performance of BSLM ( <b>U</b> Parameter)	146
5.5	Performance of BSLM ( <b>N</b> Parameter)	149
5.5.1	SNR-dependent Technique	149
5.5.2	SNR-independent Technique	160

5.6	SI and Symbol ML Decoder Integration	178
5.7	Performance of BSLM	180
5.7.1	PAPR	180
5.7.2	Complexity Reduction	182
5.8	Summary	185
<b>CHAPTER SIX: CONCLUSIONS</b>		
6.1	Conclusion	187
6.2	Future work	190
<b>REFERENCES</b>		193
<b>APPENDICES</b>		
Appendix A: Optimizing Complex Multiplication		
Appendix B: Conventional BSLM Decoding Complexity		

## LIST OF TABLES

		<b>Page</b>
Table 2.1	Summary list of all pilot-based BSLM methods in literature.	36
Table 2.2	Summary list of all data-based BSLM methods in literature.	57
Table 3.1	System parameters for simulations	78
Table 4.1	Closest constellation mapping for the unrotated constellation diagram $\mathcal{Q}$ . $d_{m,0}(v)$ denotes the index or the demodulated data of the symbol $X_{m,0}(v)$ .	100
Table 4.2	Closest constellation mapping for the rotated constellation diagram $\mathcal{Q}_1$ .	100
Table 4.3	An example of binary descrambling array for BSLM with Gray mapped 16-QAM modulation and scrambling factors $B \in \{\pm 1, \pm j\}$ .	126
Table 5.1	List of achieved DCRR values of the proposed MLPK method over the conventional BSLM decoder under different parameters.	133
Table 5.2	Comparison in terms of number of operations between PSK Phase based decoder and conventional BSLM for different modulation order $q$ .	135
Table 5.3	Comparison in terms of number of operations between PSK Phase based decoder with and without prior knowledge based decoder technique (MLPK) for different modulation order.	136
Table 5.4	Comparison in terms of DCRR over conventional BSLM between PSK Phase based decoder with and without prior knowledge based decoder technique (MLPK) for different modulation order.	137
Table 5.5	Comparison in terms of number of operations between QAM property based decoder and conventional BSLM for different modulation order $q$ .	138
Table 5.6	Comparison in terms of number of operations between QAM property-based ML decoders with and without prior knowledge based decoding technique (MLPK) for different modulation order.	140

Table 5.7	Comparison list in terms of number of operations between decoding rotated signal in rotated lattice versus un-rotated lattice for PSK property based decoder with different modulation orders.	141
Table 5.8	Comparison list in terms of number of operations between decoding rotated signal in rotated lattice versus un-rotated lattice for QAM property based decoder with different modulation orders.	142
Table 5.9	Comparison list in terms of number of operations between PSK property-based MLPK decoder with two lattices versus single lattice decoding capability.	143
Table 5.10	Comparison list in terms of number of operations between QAM property-based MLPK decoder with two lattices versus single lattice decoding capability	144
Table 5.11	Comparison list in terms of DCRR over conventional BSLM between MLPK PSK properties based decoder with two lattices versus single lattice decoding capability.	145
Table 5.12	Comparison list in terms of DCRR over conventional BSLM between MLPK QAM properties based decoder with two lattices versus single lattice decoding capability.	145
Table 5.13	ANOVA statistical hypothesis test result for SNR-dependent method.	160
Table A.1	Detailed list of maximum total number of real operations required by $q$ -PSK property based decoder for different $q$ .	
Table A.2	Detailed list of average number of real operations required by the optimized implementation of $q$ -PSK property based decoder for different $q$ .	
Table A.3	Detailed list of maximum total number of real operations required by PSK property-based MLPK decoders of different $q$ .	
Table A.4	Detailed list of average number of real operations required by optimized PSK property-based MLPK decoders of different $q$ .	
Table A.5	Detailed list of maximum total number of real operations required by $q$ -QAM property based decoder with different $q$ .	



Table A.6	Detailed list of average number of real operations required by the optimized implementation of QAM property-based ML decoders.
Table A.7	Detailed list of average number of real operations required by the optimized implementation of QAM property-based MLPK decoders.
Table A.8	Detailed list of average number of real operations required by the optimized implementation of $q$ -PSK property-based ML decoder (with two lattice decoding capability) to decode a rotated symbol.
Table A.9	Detailed list of average number of real operations required by the optimized implementation of $q$ -QAM property-based ML decoder (with two lattice decoding capability) to decode a rotated symbol.
Table A.10	Detailed list of average number of real operations required by the optimized PSK property-based MLPK decoder (with two lattice decoding capability) to decode one received symbol.
Table A.11	Detailed list of average number of real operations required by the optimized QAM property-based MLPK decoder (with two lattice decoding capability) to decode one received symbol.
Table B.1	Total number of operations required by the conventional BSLM for different modulation orders $q$ .

## LIST OF FIGURES

		Page
Figure 1.1	A brief illustration of research problems and the goal of this research.	6
Figure 2.1	An example of frequency spectrum of 8 channels for FDM and OFDM illustrated in A and B respectively(LaSorte et al., 2008).	13
Figure 2.2	An example of high peaks in OFDM due to summation of orthogonal subcarriers.	15
Figure 2.3	An example of constellation extension through modulo-D concept applied on TI approach for 4QAM modulation.	21
Figure 2.4	An example of 9 different values for mapping the symbol $1+1j$ in 4-QAM.	22
Figure 2.5	An example of dividing subcarriers into 3 disjoint groups using adjacent scheme (Müller et al., 1997).	24
Figure 2.6	An example of dividing subcarriers into 3 disjoint groups using interleaved scheme(Muller and Huber, 1997b).	24
Figure 2.7	An example of dividing subcarriers into 3 disjoint groups using pseudo-random scheme(Müller et al., 1997).	25
Figure 2.8	An example of pilot location disparity for embedding side-information with $N = 16$ , $N_p = 2$ , and $U = 4$ .	28
Figure 2.9	List of 8 possible subvectors for $M=5$ and $K=2$ used to construct the vectors of energy extension factors(Le Goff et al., 2009).	39
Figure 2.10	4-QAM vs 7-Hex Constellation(Han et al., 2008).	48
Figure 2.11	An Illustration of Adjacent and Scattered partitioning Pattern unmodified(Alsusa and Yang, 2008b).	49
Figure 2.12	An example of reshaped 4-QAM(Li et al., 2011).	53
Figure 2.13	An explanation for binary patterns of phase rotation factors for embedding SI in BSLM with $U=4$ and $L=2$ . ( $p \in \{0,1\}$ )	60
Figure 3.1	Implementation flow chart	66
Figure 3.2	BSLM phase rotation against SLM.	67

Figure 3.3	Construction of phase disparity controller $P$ for $U = 8$ and its impact on SLM symbol.	68
Figure 3.4	An illustration of conventional data based BSLM receivers' main parts.	69
Figure 3.5	Designing process of four different BSLM receivers with very low decoding complexity.	70
Figure 3.6	AWGN channel concept.	72
Figure 3.7	Magnitude of one realization of Rayleigh channel.	75
Figure 3.8	Accepting/rejecting null hypothesis using ANOVA test.	77
Figure 4.1	MLPK general block diagram	82
Figure 4.2	De-rotation effect of known PSK point.	83
Figure 4.3	De-rotation effect of known 16-QAM point	84
Figure 4.4	De-rotation effect of known 64-QAM point	86
Figure 4.5	Symmetry property in PSK modulation.	88
Figure 4.6	Symmetry property in QAM modulation.	88
Figure 4.7	16-QAM constellation diagram due to multipath effect.	89
Figure 4.8	$pskfindclosestX$ algorithm ( $q = 8$ , gray mapping)	96
Figure 4.9	$MLPKpskfindclosestX$ 's algorithm for finding $m_0 \in Q^{(0)}$ and its corresponding $m_1 \in Q_1$ for $q = 8$ .	99
Figure 4.10	$QAMfindclosestX$ flow chart illustration ( $q = 16$ , gray mapping)	102
Figure 4.11	Flow chart diagram for decoding $\mathcal{R}_{n,p}   \mathcal{R}_{n,0} \in Q^{(0)}$ in 16-QAM modulation using $MLPKQAMfindclosestX$ algorithm.	107
Figure 4.12	Minimum sub-block's active number of subcarriers per Eb/No(dB) for BSLM with $N = 256$ , $U = 4$ , and 4-QAM modulation.	110
Figure 4.13	Consistent minimum sub-block's active number of subcarriers per Eb/No(dB) for BSLM with $N = 256$ , $U = 4$ , and 4-QAM modulation.	111

Figure 4.14	<i>MLPKQAMfindclosestXp</i> 's flow chart for demodulating the received signal, corresponding to $m_0 = 8$ , in the rotated constellation diagram realm.	117
Figure 4.15	Noise margin for both rotated and unrotated 8-PSK.	119
Figure 4.16	<i>QAMDemodulateXp</i> algorithm's flow chart diagram for demodulating $\mathcal{R}_{n,0} \in \mathcal{Q}_1$ with $q = 16$ and gray mapping	122
Figure 5.1	Performance evaluation of BER of different SI sequence coding and decoding scheme (binary, orthogonal, and orthogonal-hybrid) for BSLM with $N = 256$ , $q = 4$ , and $U = 16$ under Rayleigh channel.	147
Figure 5.2	Performance evaluation of SIER of different SI sequence coding and decoding scheme (binary, conventional orthogonal-weight, and proposed orthogonal-hybrid) for BSLM with $N = 256$ , $q = 4$ , and $U = 16$ under Rayleigh channel.	147
Figure 5.3	Performance evaluation of the proposed orthogonal-hybrid decoding scheme for BSLM with $N = 256$ , $q = 4$ , and $U = 8$ under AWGN and Rayleigh channel. The ratio of soft to hard decoded SI.	148
Figure 5.4	The DCRR of addition operations achieved by the proposed orthogonal-hybrid decoding scheme per Eb/No over the conventional orthogonal-weight based metrics decoding in the conventional BSLM with $N = 256$ , $U = 8$ , and $q = 4$ .	149
Figure 5.5	Active number of subcarriers per sub-block $Z^{(SNR)}$ (forward and backward mode) vs SNR per bit for BSLM with $N = 256$ , $U = 16$ , and 16-QAM modulation under Rayleigh and AWGN channel.	150
Figure 5.6	DCRR performance of the proposed SNR-dependent technique vs SNR per bit for BSLM with $N = 256$ , $U = 16$ , and 16-QAM modulation under Rayleigh and AWGN channel.	151
Figure 5.7	BER of SNR-dependent technique for BSLM with $N = 256$ , $U = 16$ , and 16-QAM modulation under Rayleigh and AWGN channel.	152
Figure 5.8	DCRR performance of SNR-dependent technique (Forward mode) for BSLM with $N = 256$ , and 4-QAM modulation for various $U$ iteration values under Rayleigh and AWGN channel.	153

Figure 5.9	DCRR performance of SNR-dependent technique (Backward mode) for BSLM with $N = 256$ , and 4-QAM modulation for various $U$ iteration values under Rayleigh and AWGN channel.	154
Figure 5.10	DCRR performance of SNR-dependent technique (Forward mode) for BSLM with $N = 512$ , and 4-QAM modulation for various $U$ iteration values under Rayleigh and AWGN channel.	154
Figure 5.11	DCRR performance of SNR-dependent technique (Backward mode) for BSLM with $N = 512$ , and 4-QAM modulation for various $U$ iteration values under Rayleigh and AWGN channel.	155
Figure 5.12	DCRR performance of SNR-dependent technique (Forward mode) for BSLM with $N = 512$ , and $U = 16$ for various $q$ -QAM modulations under Rayleigh and AWGN channel.	155
Figure 5.13	DCRR performance of SNR-dependent technique (Backward mode) for BSLM with $N = 512$ , and $U = 16$ for various $q$ -QAM modulations under Rayleigh and AWGN channel.	156
Figure 5.14	DCRR performance of SNR-dependent technique for BSLM with $N = 512$ , and 4-PSK modulation for various $U$ iteration values under Rayleigh and AWGN channel.	157
Figure 5.15	DCRR performance of SNR-dependent technique for BSLM with $N = 512$ , and 8-PSK modulation for various $U$ iteration values under Rayleigh and AWGN channel.	157
Figure 5.16	DCRR performance of SNR-dependent technique for BSLM with $N = 512$ , and 16-PSK modulation for various $U$ iteration values under Rayleigh and AWGN channel.	158
Figure 5.17	DCRR performance of SNR-dependent technique for BSLM with $N = 512$ , and $U = 16$ for various $q$ -PSK modulations under Rayleigh and AWGN channel.	159
Figure 5.18	BER performance of different active number of sub-block's subcarriers values $Z$ for BSLM with $N = 256$ , $U = 16$ , and 64-QAM modulation under Rayleigh channel.	162
Figure 5.19	BER performance of different active number of sub-block's subcarriers values $Z$ for BSLM with $N = 256$ , $U = 4$ , and 64-QAM modulation under Rayleigh channel.	163
Figure 5.20	BER performance of different active number of sub-block's subcarriers values $Z$ for BSLM with $N = 256$ , $U = 16$ , and 16-QAM modulation under Rayleigh channel.	163

Figure 5.21	BER performance of different active number of sub-block's subcarriers values $Z$ for BSLM with $N = 256$ , $U = 4$ , and 16-QAM modulation under Rayleigh channel.	164
Figure 5.22	BER performance of different active number of sub-block's subcarriers values $Z$ for BSLM with $N = 256$ , $U = 16$ , and 4-QAM modulation under Rayleigh channel.	164
Figure 5.23	BER performance of different active number of sub-block's subcarriers values $Z$ for BSLM with $N = 256$ , $U = 4$ , and 4-QAM modulation under Rayleigh channel.	165
Figure 5.24	BER performance of different active number of sub-block's subcarriers values $Z$ for BSLM with $N = 256$ , $U = 16$ , and 16-QAM modulation under AWGN channel.	166
Figure 5.25	BER performance of different active number of sub-block's subcarriers values $Z$ for BSLM with $N = 256$ , $U = 4$ , and 16-QAM modulation under AWGN channel.	166
Figure 5.26	BER performance of different active number of sub-block's subcarriers values $Z$ for BSLM with $N = 256$ , $U = 16$ , and 4-QAM modulation under AWGN channel.	167
Figure 5.27	BER performance of different active number of sub-block's subcarriers values $Z$ for BSLM with $N = 256$ , $U = 4$ , and 4-QAM modulation under AWGN channel.	167
Figure 5.28	BER performance of different active number of sub-block's subcarriers values $Z$ for BSLM with $N = 512$ , $U = 16$ , and 16-QAM modulation under Rayleigh channel.	168
Figure 5.29	BER performance of different active number of sub-block's subcarriers values $Z$ for BSLM with $N = 512$ , $U = 4$ , and 16-QAM modulation under Rayleigh channel.	169
Figure 5.30	BER performance of different active number of sub-block's subcarriers values $Z$ for BSLM with $N = 512$ , $U = 16$ , and 4-QAM modulation under Rayleigh channel.	169
Figure 5.31	BER performance of different active number of sub-block's subcarriers values $Z$ for BSLM with $N = 512$ , $U = 4$ , and 4-QAM modulation under Rayleigh channel.	170

Figure 5.32	BER performance of different active number of sub-block's subcarriers values $Z$ for BSLM with $N = 512$ , $U = 16$ , and 16-QAM modulation under AWGN channel.	170
Figure 5.33	BER performance of different active number of sub-block's subcarriers values $Z$ for BSLM with $N = 512$ , $U = 4$ , and 16-QAM modulation under AWGN channel.	171
Figure 5.34	BER performance of different active number of sub-block's subcarriers values $Z$ for BSLM with $N = 512$ , $U = 16$ , and 4-QAM modulation under AWGN channel.	171
Figure 5.35	BER performance of different active number of sub-block's subcarriers values $Z$ for BSLM with $N = 512$ , $U = 4$ , and 4-QAM modulation under AWGN channel.	172
Figure 5.36	BER performance of different active number of sub-block's subcarriers values $Z$ for BSLM with $N = 256$ , $U = 16$ , and 8-PSK modulation under Rayleigh channel.	174
Figure 5.37	BER performance of different active number of sub-block's subcarriers values $Z$ for BSLM with $N = 256$ , $U = 4$ , and 8-PSK modulation under Rayleigh channel.	174
Figure 5.38	BER performance of different active number of sub-block's subcarriers values $Z$ for BSLM with $N = 256$ , $U = 16$ , and 8-PSK modulation under AWGN channel.	175
Figure 5.39	BER performance of different active number of sub-block's subcarriers values $Z$ for BSLM with $N = 256$ , $U = 4$ , and 8-PSK modulation under AWGN channel.	175
Figure 5.40	BER performance of different active number of sub-block's subcarriers values $Z$ for BSLM with $N = 512$ , $U = 16$ , and 8-PSK modulation under Rayleigh channel.	176
Figure 5.41	BER performance of different active number of sub-block's subcarriers values $Z$ for BSLM with $N = 512$ , $U = 4$ , and 8-PSK modulation under Rayleigh channel.	177
Figure 5.42	BER performance of different active number of sub-block's subcarriers values $Z$ for BSLM with $N = 512$ , $U = 16$ , and 8-PSK modulation under AWGN channel.	177

Figure 5.43	BER performance of different active number of sub-block's subcarriers values $Z$ for BSLM with $N = 512$ , $U = 4$ , and 8-PSK modulation under AWGN channel.	178
Figure 5.44	CCDF Performance of PAPR of SLM with different phase rotation set due to blind or no blind SLM for $N = 256$ , $U = 16$ , and 16-QAM.	181
Figure 5.45	CCDF Performance of PAPR of SLM with different phase rotation set due to blind or no blind SLM for $N = 256$ , $U = 16$ , and 64-QAM.	181
Figure 5.46	DCRR performance of joint MLPK decoder with SNR-dependent method in terms of $ \cdot ^2$ operations for BSLM with 4-QAM modulation and various settings.	183
Figure 5.47	DCRR performance of joint MLPK decoder with SNR-dependent method in terms of $ \cdot ^2$ operations for BSLM with 16-QAM modulation and various settings.	183
Figure 5.48	DCRR performance of joint MLPK decoder with SNR-dependent method in terms of $ \cdot ^2$ operations for BSLM with 64-QAM modulation and various settings.	184
Figure 5.49	DCRR performance of joint MLPK decoder with SNR-dependent method in terms of $ \cdot ^2$ operations for BSLM with 8-PSK modulation and various settings.	184



## LIST OF ABBREVIATIONS

ACE	Active Constellation Extension
AWGN	Additive White Gaussian Noise Channel
ANOVA	Analysis of Variance
BER	Bit Error Rate
SER	Symbol Error Rate
SIER	Side-Information Error Rate
CCDF	Complementary Cumulative Distribution Function
CDF	Cumulative Distribution Function
CP	Cyclic Prefix
CM	Conversion Matrix
DCRR	Decoding Complexity Reduction Ratio
DC-MF	Delayed Correlation with Matched Filter
DCT	Discrete Cosine Transform
DFT	Discrete Fourier Transform
DSL	Digital Subscriber Line
DST	Discrete Sine Transform
FDM	Frequency Division Multiplexing
FFT	Fast Fourier Transform
HPA	High Power Amplifier
ICI	Inter-Carrier Interference
IDCT	Inverse Discrete Cosine Transform
IDFT	Inverse Discrete Fourier Transform

IDST	Inverse Discrete Sine Transform
IFFT	Inverse Fast Fourier Transform
JROF	Joint Rotation and Offset
IQRC	In-phase and Quadrature Recombination
ISI	Inter-Symbol Interference
MMSE	Minimum Mean Square Error
ML	Maximum likelihood
MLPK	ML decoder with prior knowledge
OFDM	Orthogonal Frequency Division Multiplexing
PA	Power Amplifier
HPA	High Power Amplifier
PAPR	Peak-to-Average Power Ratio
PTS	Partial Transmit Sequence
QAM	Quadrature Amplitude Modulation
SLM	Selected Mapping
H-SLM	Hexagonal-SLM
R-SLM	SLM with Reshaping technique
SNR	Signal-to-Noise Ratio
TDSC	Time Domain Symbol Combining
TI	Tone Injection
TR	Tone Reservation

# **PENAMBAHBAIKAN SLM BUTA DENGAN PENGURANGAN KERUMITAN PENYAHKODAN UNTUK SISTEM OFDM**

## **ABSTRAK**

SLM adalah teknik pengurangan (PAPR) yang terkenal yang mampu mengurangkan PAPR sistem dengan berkesan tanpa mengganggu isyarat. Walau bagaimanapun, SLM menyebabkan masalah kehilangan kadar data disebabkan oleh keperluan untuk menghantar indeks lelaran terpilih kepada penerima sebagai maklumat sampingan. Untuk menyelesaikan masalah ini, banyak kaedah (BSLM) dicadangkan dalam kesusasteraan. Kaedah BSLM membenamkan maklumat sampingan dalam kedua-dua perintis atau isyarat data menggunakan fasa atau perbezaan bentuk tenaga, oleh itu penerima boleh secara terus menyahkodkan isyarat menggunakan penyahkodan (ML). Dalam kajian ini, skema BSLM berasaskan data yang berbeza dengan kerumitan penyahkodan yang sangat rendah dicadangkan untuk modulasi QAM dan PSK. Skim BSLM yang dicadangkan dibahagikan kepada tiga peringkat utama untuk parameter sistem yang berlainan ( $q$ ,  $N$ , dan  $U$ ). Peringkat pertama ditangani dengan memperkenalkan ML dengan konsep pengetahuan sebelumnya (MLPK). Kemudian, ciri-ciri baru yang dioptimumkan berasaskan pengubahsuaian MLPK untuk modulasi PSK dan QAM di mana kerumitan penguraian BSLM dikurangkan oleh operasi  $(q - 1)/q |\cdot|^2$ . Pendekatan yang dicadangkan seterusnya (kaedah SNR-bebas dan kaedah SNR-bergantung) menangani masalah sejumlah besar sub-pembawa untuk dua senario ketersediaan maklumat SNR isyarat yang diterima. Nisbah pengurangan kerumitan penyahkodan (DCRR) ditetapkan untuk SNR bebas, walau bagaimanapun, ia berbeza berdasarkan maklumat SNR untuk kaedah SNR-bergantung dan oleh itu

kaedah SNR-bergantung kepada dapat mencapai maksimum DCRR  $(N - L) / N$  pada nilai SNR yang tinggi. Kerumitan peringkat terakhir ditangani menggunakan proses estimasi SI hibrid bi-ortogonal. Semua kaedah pengurangan kerumitan yang dicadangkan yang berkaitan dengan sama ada parameter sistem  $q$  atau  $N$  mengurangkan kerumitan penyahkodan BSLM dengan ketara. Walau bagaimanapun, reka bentuk BSLM terakhir yang menggunakan gabungan semua kaedah yang dicadangkan mencapai DCRR yang sangat ketara berbanding BSLM konvensional. Kaedah penyelenggaraan kaedah SNR -bergantung dengan pengubahsuaian MLPK berasaskan ciri-ciri yang ditingkatkan, misalnya, mencapai DCRR 99.9% berbanding BSLM konvensional pada SNR setiap bit 11 dB (AWGN) dan 22 dB (Rayleigh) untuk  $N = 512$ ,  $q = 4$ , dan  $U = 4$  di bawah AWGN. Akhir sekali, satu fasa baru berasaskan binari, proses putaran dicadangkan untuk menghapuskan proses demodulasi simbol selepas proses pengekodan SI. Oleh itu, reka bentuk penerima BSLM yang dicadangkan mempunyai kerumitan yang lebih rendah walaupun dibandingkan dengan SLM konvensional pada nilai SNR yang tinggi.

# AN IMPROVED BLIND SELECTED MAPPING WITH DECODING COMPLEXITY REDUCTION FOR ORTHOGONAL FREQUENCY DIVISION MULTIPLEXING SYSTEM

## ABSTRACT

SLM is a well-known peak-to-average power ratio (PAPR) reduction technique that is capable of effectively reducing the system's PAPR without distorting the signal. However, SLM causes a data rate loss issue due to the necessity for sending the selected iteration index to the receiver as side-information. To solve this issue, many blind SLM (BSLM) methods have been proposed in the literature. Such BSLM methods embed side-information in either pilot or data signals using phase or energy disparity forms. Hence, the receiver can blindly decode the signals using a maximum likelihood (ML) decoder. In this research, different data-based BSLM schemes with very low decoding complexity are proposed for both QAM and PSK modulation. The proposed BSLM schemes are broken down into three main stages for different system parameters ( $q$ ,  $N$ , and  $U$ ). The first stage is addressed by introducing the concept of the maximum likelihood with prior knowledge (MLPK). Then, new optimized property based MLPK decoders are derived for PSK and QAM modulations where the BSLM decoding complexity is reduced by  $(q - 1)/q$   $|\cdot|^2$  operations. The next proposed approaches (SNR-independent and SNR-dependent methods) address the problem concerning the large number of subcarriers for two scenarios of SNR information availability of the received signal. The performance of the decoding complexity reduction ratio (DCRR) is fixed for the SNR-independent method. However, it varies based on the SNR information for the SNR-dependent method, and hence, the SNR-dependent method can achieve the maximum DCRR of  $(N - L)/N$

at high SNR values. The complexity of the last stage is addressed using a biorthogonal-hybrid SI estimation process. All proposed complexity reduction methods pertaining to either  $q$  or  $N$  system parameter reduce the BSLM decoding complexity significantly. However, the final BSLM designs using a combination of all proposed methods achieve a very significant DCRR over the conventional BSLM. The joint implementation of the SNR-dependent method with the enhanced property-based MLPK decoder, for instance, achieved a DCRR of 99.6% over the conventional BSLM at SNR per bit of 11 dB(AWGN) and 22 dB(Rayleigh) for  $N = 512$ ,  $q = 4$ , and  $U = 16$ . Finally, a new simple binary-based phase de-rotation process is proposed to eliminate the symbol demodulation process that is due after the SI decoding process. Hence, the proposed BSLM receiver designs have lower complexity even compared to the conventional SLM at high SNR values.

# CHAPTER ONE

## INTRODUCTION

### 1.1 Background

In the earlier time of wireless communication, single carrier modulation (SCM) was a revolutionary by itself in which the data pulses are carried using a single carrier. The single carrier modulation (SCM) was able to increase the speed of data transmission by reducing the symbol duration, thus increasing the symbol rate. However, as the symbol duration decreases, the transmitted symbols start to drastically overlap each other at the receiver. This is due to the multipath effect, which introduces the issue of the inter-symbol interference (ISI). To alleviate the ISI issue, SCM requires the implementation of a very complex equalizer.

To solve the speed limitation of SCM, a parallel transmission concept was adopted using multi-tone multiplexing techniques such as frequency division multiplexing (FDM) and orthogonal frequency division multiplexing (OFDM). However, unlike FDM where channels are non-overlapping each other, OFDM, with the help of the orthogonality feature, uses densely packed and overlapping/non-interfering channels to efficiently utilize the bandwidth. In fact, OFDM divides its channel into multiple narrow band sub-channels to gain robustness over the frequency selective fading channel and eliminate the adjacent subcarrier crosstalk (Mathworks). The carrier of each sub-channel is called subcarrier and the subcarriers are orthogonal to each other.

OFDM does not only increase the data transmission rate through multiplexing techniques, but it also eradicates the ISI effect easily using a cyclic prefix (CP), of length exceeds the maximum spread delay of the multipath channel, and a very simple equalizer. The cyclic prefix with the appropriate length makes channel estimation and equalization simpler in OFDM.

Although OFDM sounds an interesting modulation technique, it was not until the advances in the DSP technology that OFDM received an immense interest in application design. Thanks to the discrete Fourier transform (DFT) and its fast implementation algorithm FFT, an orthogonality feature is maintained and all subcarriers are modulated/demodulated at once using a single fast Fourier transform function (FFT) at both transmitter and receiver. Nowadays, OFDM is a very popular technique that forms the basis of many famous applications and standards such as WLAN, ADSL, DVB-T, and LTE.

Although OFDM increases the data transmission rate efficiently and it is robust to channel impairments, its signal suffers from the high peak to average power ratio (PAPR). The summation of multiple orthogonal subcarriers constructs some very high peaks. The problem related to the high peaks of the OFDM signal cannot be amplified linearly using simple high power amplifier (HPA) as the peaks fall down in the saturation/non-linear region of the amplifier, thus distorting the amplified signal and causing in-band and out-band radiations. To prevent such signal distortion, a very complex power amplifier design with back-off is required. However, this solution is power inefficient and complex at the same time.



There are many techniques that have been proposed in the literature to alleviate the PAPR issue. The proposed PAPR reduction techniques can be categorized into two main categories: distortion and distortion-less techniques. The distortion PAPR reduction techniques such as clipping degrade the BER performance of the system. Clipping technique, for instance, provides a simple but inefficient solution. On the other hand, the distortion-less PAPR reduction techniques maintain the BER performance of the system under certain criteria. Examples of distortion-less techniques are PTS, SLM, TI, TR, ACE and coding (Rahmatallah and Mohan, 2013).

## **1.2 Problem Statement**

SLM is a well-known PAPR reduction technique, which is also considered a distortion-less PAPR reduction technique (Le Goff et al., 2009). The SLM achieves PAPR reduction by simply iterating different scrambling operations guided by  $U$  scrambling vectors and selecting one of the emerged/reformed signals with the best PAPR value for transmission. However, in order for the receiver to be able to decode the received signal and inverse the scrambling process conducted at the transmitter side, the sender needs to send the index of the selected iteration of the transmitted signal as side-information. Furthermore, since side-information has a critical status as it impacts the process of recovering the original signal at the receiver, it might be necessary to apply some coding on Side-information before transmission in order to maintain the BER of the system.

Side-information and its coding redundancy bits cause a data rate loss issue (Rahmatallah and Mohan, 2013). The system data rate is valuable, especially in

wireless, and therefore, many blind SLM (BSLM) schemes with blind receivers have been proposed in the literature to eliminate the needs for sending side-information and its coding redundancy bits, and hence save the system data rate and maintain the OFDM efficiency. Blind SLM techniques simply implement a disparity concept to embed side-information in the signal, and the receiver implements a maximum likelihood decoder in most cases to decode/estimate the embedded side-information.

In BSLM, Side-information can be embedded in pilots or data subcarriers. The pilot-based BSLM, for instance, embeds the SI into pilot subcarriers, and since pilots' complex symbols are known in prior to the receiver the SI estimation process is simple in general. However, efficient channel estimation methods does not transmit pilots every transmission to save bandwidth. Hence, pilot-based BSLM schemes cannot apply PAPR reduction process when pilots are not available, and as a result, the PAPR reduction performance is degraded.

Some pilot-based BSLM schemes suggests that in a system where pilots are available every  $V$  frame, the data sequence of  $V$  frame should be queued and then be processed at once using a modified selecting function. The modified selecting function finds the iteration index of the minimum total PAPR value of  $V$  processed data sequences instead of the minimum PAPR value of each processed data sequence. Although this technique improves the PAPR reduction performance of pilot-based BSLM, the BSLM needs to wait for the data sequences of  $V$  frames to be collected before starting the process. Moreover, any error in estimating SI will affect the data recovery of  $V$  frames instead of single frame. Furthermore, the PAPR reduction performance is still degraded compared to that of SLM.

Since pilot-based BSLM lacks the availability of pilots in every OFDM frame, many data-based BSLM methods have been proposed to maintain the PAPR reduction capability of SLM. Data-based BSLM schemes embeds SI in data subcarriers. And due to the fact that the decoding complexity is dependent on the number of used subcarriers for embedding SI and the modulation order, the decoding complexity of data-based BSLM schemes is very high and prohibitive, in general, compared to that of pilot-based BSLM schemes.

Since data-based BSLM schemes does not degrade the PAPR reduction performance of SLM, data-based BSLM is a favorable solution if decoding complexity at the receiver is kept reasonable and the system BER is not degraded. Therefore, this study investigate the problem of high decoding complexity on data-based BSLM receivers and focus on the development of very low complex data-based BSLM receivers while maintaining the BER of the system.

First, the conventional data-based BSLM in (Joo et al., 2012) is analyzed and divided into three main blocks where the complexity of each block is dependent on single system parameter (i.e. modulation order  $q$ , number of subcarriers  $N$ , or number of maximum iteration  $U$ ). Then, the high complexity and the complexity dependency on system's parameters of each block is addressed separately before a joint BSLM designs are proposed for further significant complexity reduction.

Then, for further decoding complexity reduction at the receiver, the  $N$  complex symbol descrambling operations are replaced by simple binary descrambling operations and the last  $N$  symbol demodulation process is eliminated by integrating the process into BSLM decoder. As a result, this research will eventually achieve four efficient designs of BSLM receivers with very low decoding complexity that address two different modulations and two different implementation scenarios. Figure 1.1 gives an insight about the problems that this research work herein aims to address and solve.

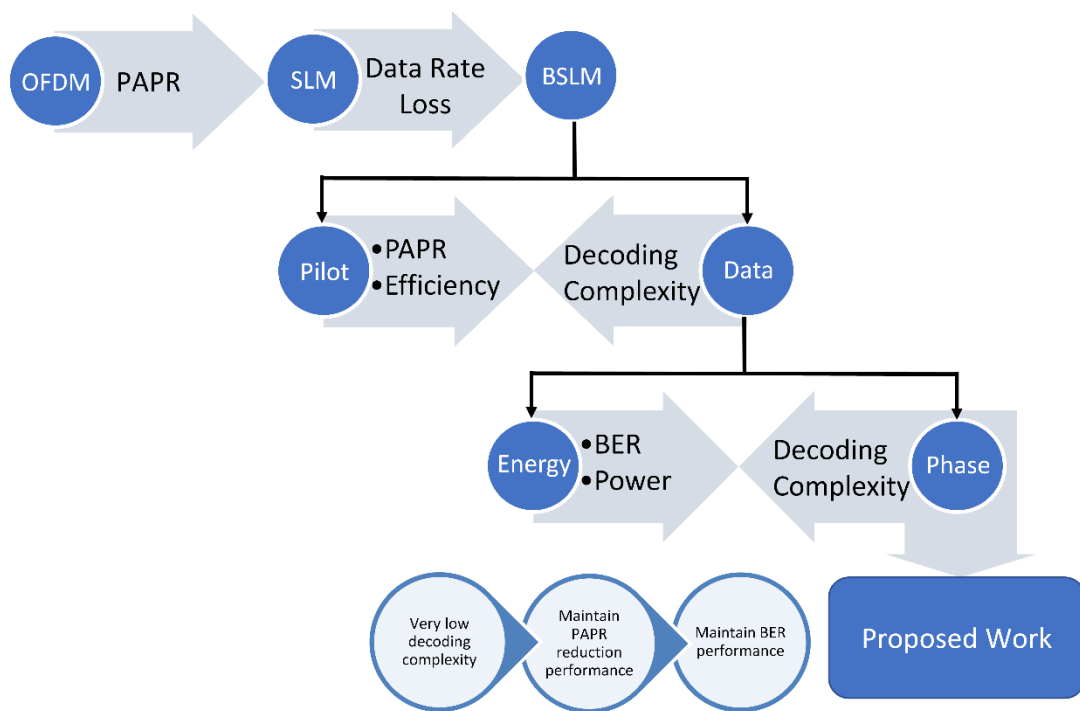


Figure 1.1 A brief illustration of research problems and the goal of this research.

### 1.3 Objectives

This research aims to reduce the decoding complexity of the data-based BSLM receiver very significantly, and accordingly achieve the following specific research objectives:

- 1- To develop four efficient designs of blind SLM receivers for solving the SLM data rate loss issue efficiently. The four designs will target two types of modulations and two implementation scenarios.
- 2- To reduce the side-information decoding complexity and solve the problem of complexity dependency on  $q$ ,  $N$ , and  $U$  parameters.
- 3- To reduce the overall decoding complexity of the proposed BSLM schemes.

### 1.4 Project Scope

This research focuses on solving the data rate loss issue of the conventional SLM scheme. The data rate loss issue is solved by proposing different blind SLM schemes in which the receiver of each proposed BSLM design is blindly inverting the scrambling operations conducted on the signal at the transmitter. The performance of the proposed blind SLM schemes is also studied in terms of PAPR, bit error rate (BER), and decoding complexity reduction ratio (DCRR).

The proposed blind SLM schemes are evaluated in simulation using MATLAB. The MATLAB software is used to simulate the proposed methods and collect BER results under various settings to evaluate the BER performance of the proposed methods pertaining  $N$  and  $U$  parameters as both parameters based methods are derived

and designed based on hypothesis. The performance of the proposed blind SLM schemes is analyzed for two modulation schemes (QAM and PSK), two different number of subcarriers (256, 512), and three different modulation orders (4, 8, and 16 for PSK and 4, 16, and 64 for QAM). The QPSK (4-PSK), 16-QAM, and 64-QAM modulations are very common modulation types and they are used in many applications and standards, e.g. 802.11n (Frenzel, 2012). Hence, they are used in evaluating the proposed methods in this thesis, however, other modulation orders are used in evaluation as well to show the effect of modulation order changes on DCRR performance of the proposed BSLM receivers. The two number of subcarriers ( $N = 256$  and  $N = 512$ ) are used in evaluation to show and study the influence of the changes in the parameter  $N$  on the performance of the proposed methods. Furthermore, the BER performance of the proposed schemes is analyzed under different channels (i.e. AWGN and Rayleigh channels). For the Rayleigh channel, perfect channel estimation is assumed as channel estimation is beyond the scope of this thesis.

The limitation of the proposed data based BSLM receivers are the same as the limitation of data based BSLM receivers in general. For instance, the performance of phase-based data-based BSLM receivers suffers in OFDM systems with very low number of subcarriers especially at very SNR values. Therefore, in OFDM system with very low number of subcarriers it is better to encode SI and send it explicitly when the system is operating in a very noisy channel.

## 1.5 Thesis Outlines

This thesis is organized in six main chapters. The first chapter provides an introduction about OFDM, PAPR issue, PAPR reduction techniques, and the data rate loss issue of SLM method. It also presents the research objectives and scope of work. Then, an extensive review of the literature on the available PAPR reduction techniques and blind SLM schemes is conducted and presented in CHAPTER Two. The literature review list all available BSLM methods in literature and categorize them into two main category based on the mean used to embed the SI (i.e. pilots or data subcarriers). Then, each category is discussed thoroughly and summarized at the end of its category section before a final conclusion is drawn at the end of the chapter.

Next, the research methodology is discussed in details in CHAPTER Three where the general implementation flowchart for achieving research goals, evaluation terms and simulation parameters are presented and explained in details. Then, the proposed methods and concepts for designing and deriving different BSLM receivers with very low decoding complexity that address different modulation types and exploits different implementation scenarios are presented in CHAPTER Four.

The performance of the proposed complexity reduction methods is discussed in CHAPTER Five, mainly, in relation to DCRR over the conventional data based BSLM method. Also, the BER performance of the proposed methods are presented and discussed in comparison with the conventional BSLM method so that the trade-off concept used by the proposed SNR-independent method and the compromise between the DCRR and BER are illustrated clearly.

CHAPTER Six provides conclusions drawn from the study. Furthermore, some recommendations and guidance are listed in future works to either improve the proposed methods or to further study the proposed concepts. Finally, further clarifications on how the numbers of operations are calculated for each method in Chapter Five are discussed and presented in Appendices.



## CHAPTER TWO

### LITERATURE REVIEW

#### 2.1 Introduction

This chapter starts with a brief insight on orthogonal frequency division multiplexing (OFDM) technique. Then, OFDM's major problem of high peak-to-average power ratio (PAPR) is discussed along with solution requirements. The discussion about PAPR problem elaborates on measuring and evaluating the OFDM system in terms of PAPR. Furthermore, the criteria by which someone can prefer one PAPR reduction method over another is listed. Next, background information about the PAPR reduction techniques is provided with a detailed discussion about the advantageous and disadvantageous of each technique.

Among all PAPR reduction techniques, the selected mapping (SLM) technique is a well-known PAPR reduction technique for its PAPR reduction capability. However, conventional SLM method introduces data rate loss due to side-information requirements at receiver. Therefore, many blind SLM techniques were proposed in literature to tackle this problem of SLM. The proposed blind SLM techniques in the literature are discussed thoroughly in section 2.5. As blind SLM techniques can be categorized into two main categories based on the carrier of the embedded side-information (pilots or data), the discussion is carried on for each category in sub-sections 2.5.1 and 2.5.2. The advantageous and disadvantageous of both pilot based and data based blind SLM methods are discussed in details. Finally, this chapter ends with a summary of major topics covered in this chapter.

## 2.2 OFDM

Orthogonal frequency division multiplexing technique (OFDM) is an interesting multi-tone modulation technique that found its way to broad line of standards and applications that seeks for high data rate, spectral efficiency, robustness against ISI and fading, and design simplicity. The adoption of OFDM as a transmission technique is rapidly growing, and some examples of OFDM based transmission standards includes DVB, DAB, DSL, IEEE 802.11a/g, WiMax, and LTE(Rahmatallah and Mohan, 2013).

As the full name implies, the two main basis concept of OFDM are orthogonality feature and parallel transmission through multiplexing technique. Both OFDM and frequency division multiplexing (FDM) technique are capable of achieving higher data rate, compared to single carrier technique, through parallel transmission of data using multiple carriers. However, unlike FDM, OFDM can achieve the same high data transmission rate as FDM with almost half the bandwidth. In other words, with the help of orthogonality, OFDM can achieve almost double the data rate of what can be achieved in FDM using the same bandwidth. This is due to densely packing multiple subcarriers as shown in Figure 2.1. Therefore, OFDM is regarded as a bandwidth or spectral efficient modulation technique.

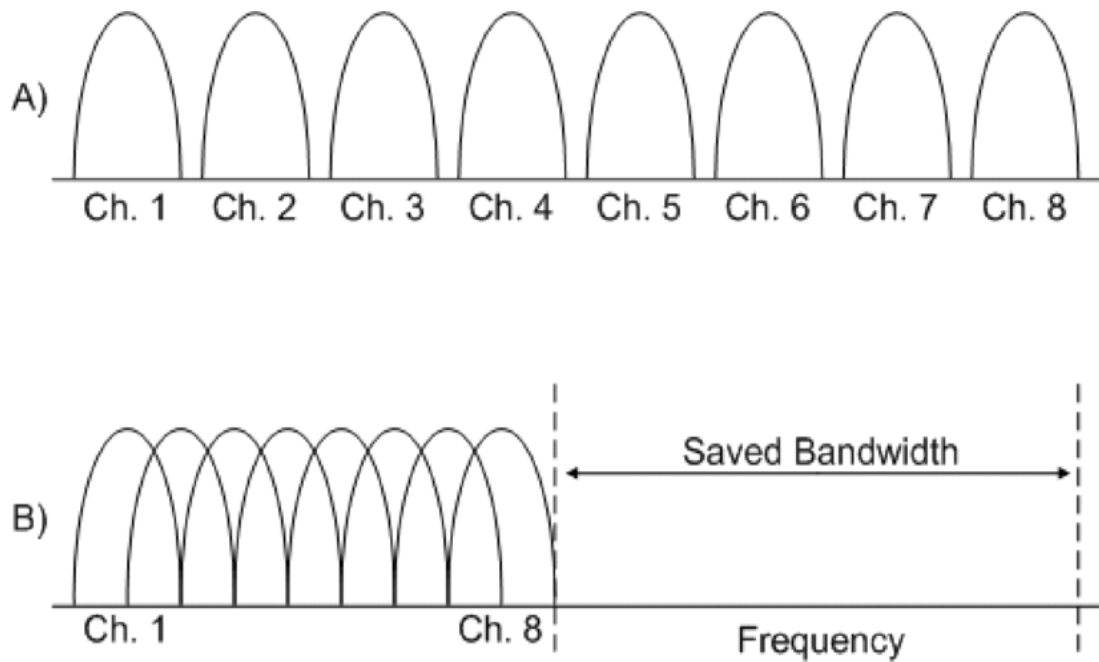


Figure 2.1 An example of frequency spectrum of 8 channels for FDM and OFDM illustrated in A and B respectively(LaSorte et al., 2008).

It is interesting to see how the subcarriers in OFDM are so densely packed to the point where they overlap each other but with no interference due to Orthogonality feature. If for any reason orthogonality between subcarriers is broken, the subcarriers will interfere with each other and the receiver will not be able to recognize the transmitted data. Therefore, orthogonality is a very important aspect of OFDM, and it was not as easy as now to maintain when the concept was introduced in the mid of 1960s(Chang, 1966, Saltzberg, 1967, LaSorte et al., 2008, Weinstein, 2009). It is only due to the advances in digital signal processing (DSP) techniques and manufacturing processes that OFDM is a very popular nowadays despite the fact that this technique was introduced in the mid of 1960s. In fact, the introducing of discrete fourier transform DFT-based OFDM and the fast fourier transform FFT-based OFDM later led to significant complexity reduction of OFDM implementation.

Beside the high spectral efficiency, OFDM has many other advantages. By sending data on multiple low rates of OFDM subcarriers' symbol in parallel simultaneously and applying the cyclic prefix technique, OFDM can achieve higher data rate and eliminate inter-symbol interference (ISI) at the same time without the need of a complex equalizer. As a result, a low complex receiver can be designed.

In general, the main advantages of OFDM can be summarized as follows(Narasimhamurthy et al., 2010):

1. High data rate
2. High spectral efficiency due to orthogonality which eliminate the guard bands used in FDM.
3. Ability to cope with severe channel conditions
4. High robustness against ISI, and fading

Despite the amazing merits of OFDM, the OFDM signal suffers from high peak to average power ratio (PAPR) problem due to the summation of all OFDM subcarriers' signals in time domain as shown in Figure 2.2. In fact, high PAPR is the major problem in OFDM because the high peaks of OFDM signal will normally fall in the saturation area instead of the linear area of the high power amplifier (HPA) which, in turns, leads to signal distortion, in-band and out-band radiation as a result of nonlinear amplification of the OFDM signal.

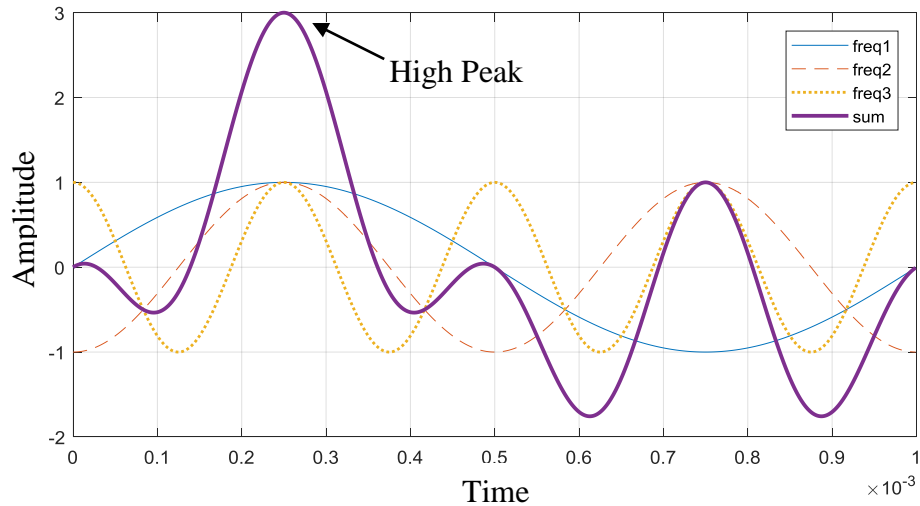


Figure 2.2 An example of high peaks in OFDM due to summation of orthogonal subcarriers.

Although it is costly and power inefficient, a very complex HPA design with back-off is required to maintain the linearity of the OFDM signal. To alleviate such problems, many PAPR reduction schemes were proposed in literature. However, each PAPR reduction scheme has an advantages and disadvantages over each other.

SLM, for instance, is a distortion-less phase rotation based PAPR reduction technique that does not increase the average transmitted power and does not affect the system BER. SLM iterates  $U$  different phase rotation sequences to emerge new alternative OFDM signal with an acceptable low PAPR. However, as SLM requires the information about the iteration index to be available at the receiver in order to correctly reverse the phase rotation operation on the received signal, SLM needs to dedicate at least  $\lceil \log_2 U \rceil$  bits for SLM side-information. Since the correctness of the received side information at the receiver is crucial for correctly un-distorting the received signal the SLM encode the side-information. The protection of side-information through encoding will increase the system data rate loss further.

The demands for increasing data rate in communication is very high, therefore every bit is a valuable information resource. Solving the OFDM PAPR issue by or with sacrificing some data rate loss is something undesirable, and researchers pushing hard to save every bit for data only. Maintaining system data rate does not only maintain the performance of system's transmission data rate but also may save some operating cost.

This literature review will mainly discuss all proposed SLM approaches without side-information in order to draw a clear picture about the contribution of the proposed works in this thesis. But let's first discuss PAPR and PAPR reduction techniques in general beforehand.

### 2.3 Peak-to-Average Power Ratio (PAPR)

PAPR is the ratio between the peak power of OFDM signal in time domain to its average power. Mathematically, let's consider the OFDM complex symbol data  $X = \{X_n | 0 \leq n \leq N - 1\}$  at frequency domain where  $X_n$  is the  $q$ -ary modulated complex symbol for the  $n$ -th subcarrier. The OFDM discrete time domain signal can be calculated using the discrete inverse fourier transform function shown in (2.1)(Han and Lee, 2005)

$$x(t) = \frac{1}{\sqrt{N}} \sum_{k=0}^{N-1} X_k \cdot e^{-j2\pi k \Delta f t}, 0 \leq t < T \quad (2.1)$$

where  $\Delta f$  is the spacing between two adjacent subcarriers, and  $x(t)$  is the discrete OFDM signal at time domain. The OFDM L oversampled discrete time domain signal is given by the equation

$$x_n = \frac{1}{\sqrt{NL}} \left( \sum_{k=0}^{N/2-1} X_k \cdot e^{-\frac{j2\pi kn}{NL}} + \sum_{k=N/2}^{NL-1} X_k \cdot e^{-\frac{j2\pi kn}{NL}} \right), 0 \leq n \leq NL - 1 \quad (2.2)$$

where  $x_n$  is the n-th signal value at time domain. The PAPR of OFDM signal is defined mathematically for (2.2) as following (Han and Lee, 2005):

$$PAPR = \frac{\text{Max}|x_k|^2}{E[|x_k|^2]} \quad ; k = 0, \dots, NL - 1 \quad (2.3)$$

where  $E[|\cdot|]$  denotes expectation and L is the oversampling value.

In order for the PAPR calculation in (2.3) to be as accurate as the PAPR of the OFDM continuous time domain signal, the PAPR has to be calculated for an oversampled OFDM signals in order not to miss any peaks that may disappear due to low number of sampling. In literature, PAPR can be accurately calculated when the oversampling factor  $L \geq 4$ , and the recommended oversampling value is  $L = 4$  (Cho et al., 2010, Han and Lee, 2005).

There are many PAPR reduction techniques have been proposed for OFDM in literature. To evaluate the performance of any proposed PAPR reduction scheme in terms of PAPR reduction, the statistical CDF or CCDF function is used. The cumulative distribution function (CDF) for  $PAPR_o$  value is given by

$$\text{CDF}(PAPR_o) = \Pr(PAPR \leq PAPR_o) \quad (2.4)$$

On the other hand, the complementary cumulative distribution function (CCDF) is calculated by the formula

$$\begin{aligned} \text{CCDF}(PAPR_o) &= 1 - \text{CDF}(PAPR_o) \\ &= \Pr(PAPR > PAPR_o) \end{aligned} \tag{2.5}$$

The PAPR reduction schemes are not only evaluated by the CCDF of PAPR. There are various important criteria that should be studied, as well, before preferring one technique over another. Some of the aspects the designer need to consider before selecting one PAPR reduction technique over another are listed below(Jiang and Wu, 2008):

- Complexity: Complexity is a very important thing to consider before selecting a PAPR reduction technique since it affects the system cost, speed, and or the space of hardware implementations directly. Some PAPR Reduction has the ability to reduce PAPR significantly but with very high complexity. Therefore, the reduction of cost due to PAPR reduction should be compared with the increase of the cost due to complexity growth.
- Data Rate Loss: In communication, the demands of increasing data rate are very high, and the loss in data rate is undesirable and should be eliminated. Therefore, data rate loss is another very important aspect of evaluating PAPR reduction schemes. Data rate loss could be a result of reserving some subcarriers for PAPR reduction or side information.
- BER: What is the benefit of simple and significant PAPR reduction techniques if BER is degraded too much. Clipping, for instance, is a simple PAPR



reduction technique but it degrades the BER at the receiver. Therefore, the performance in terms of BER should also be considered while studying any PAPR reduction technique.

- **Increase of Average Power:** The power efficiency should be considered in any PAPR reduction design. If the PAPR reduction technique increases the transmitted average power of the transmitted signal, the BER performance will be degraded when the transmitted signal is normalized back to the original power signal.

## 2.4 PAPR Reduction

There are some PAPR reduction techniques that have been proposed in literature to solve or alleviate the consequential issues of signal's high PAPR in OFDM system. The PAPR reduction techniques may be categorized, based on BER influential behaviour, as distortion or distortion-less techniques.

As the name of category implies, distortion techniques apply irreversible distortion operations on the signal form so that the distortion effect cannot be reversed at the receiver. A simple example of distortion techniques is clipping techniques in which the signal is insured not to exceed a predetermined envelope level  $A$  through clipping conducted as following(O'neill and Lopes, 1995)

$$\bar{x}(t) = \begin{cases} x(t), & |x(t)| \leq A \\ A, & x(t) > A \\ -A, & x(t) < -A \end{cases} \quad (2.6)$$

The distortion of OFDM signal due to clipping does not only degrade system BER performance but also reduces OFDM spectral efficiency as a result of the produced out-of-band radiations. The problem of spectral efficiency can be solved by filtering out the out-of-band noise, however high peaks will regrow in result(Li and Cimini, 1997, Armstrong, 2001). Iterative clipping and filtering can be used to remove out-band interference and reduce peaks regrow issue, however, complexity is increased(Armstrong, 2002).

On the other hand, distortion-less techniques apply a reversible distortion operation on the signal so that if channel status is healthy, the original signal can be retrieved at the receiver by removing the operation effect through reversing the distortion operation conducted on the signal. Distortion-less PAPR reduction technique may apply addition, extension, multiplication or scrambling operations to emerge a new alternative signal with a good PAPR value. There are various distortion-less techniques proposed in literature for PAPR reduction such as TR, TI, ACE, PTS, SLM and coding.

In tone reservation technique (TR), some subcarriers are reserved and utilized for peak reduction through the process of tone injection(Tellado and Cioffi, 1998b, Tellado and Cioffi, 1998a, Park et al., 2003, Wattanasuwakull and Benjapolakul, 2005, Yang, 2007). Since the PAPR value of OFDM signal depends on the phase and the magnitude of all OFDM sub-signals, adding the right phase and magnitude will cancel some high peaks and reduce the PAPR value in result. Therefore, TR will iterate different tones injection and select the resultant signal with minimum PAPR value. The main drawback of this technique is the increases of transmitted signal's

average power and the data rate loss due to the process of injecting tones and reserving subcarriers for PAPR reduction only.

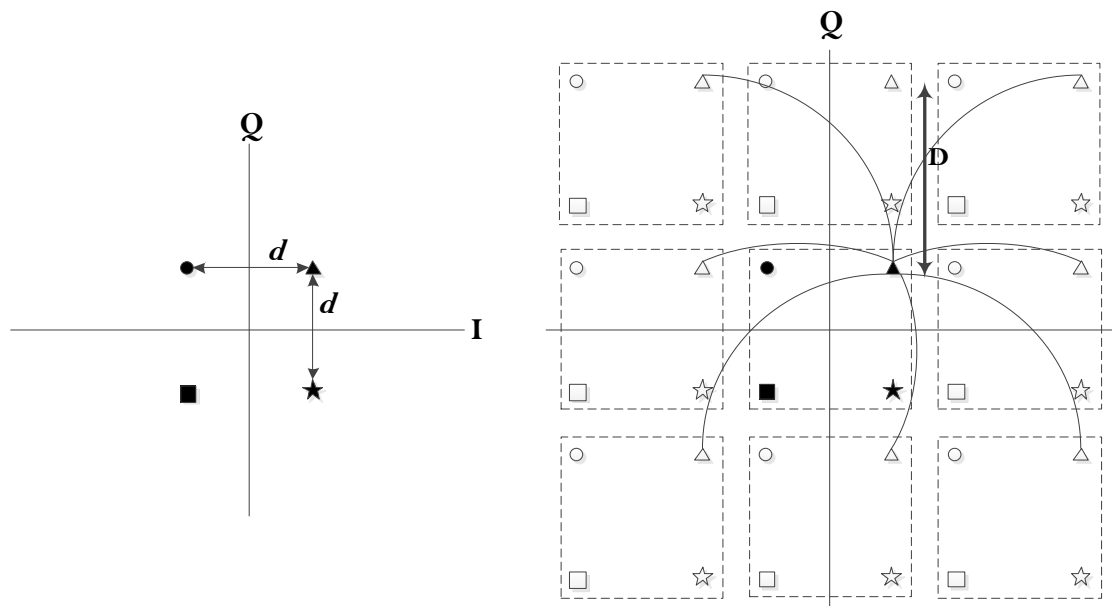


Figure 2.3 An example of constellation extension through modulo-D concept applied on TI approach for 4QAM modulation.

On the other hand, tone injection technique (TI) solves the issue of data rate loss in TR by injecting the tones  $C = [C_0, C_1, \dots, C_{N-1}]$  into data subcarriers (Tellado and Cioffi, 1998b, Hwang, 2001). However, for the injected tones to be reversed at the receiver, TI restricts injected tone values to modulo-D conditions, as shown in Figure 2.3, or mapping. In other words, as illustrated in Figure 2.4, the result of the modulo-D operation of the resultant value  $(X_n + C_n)$  has to be the original symbol  $X_n$ . As a result, TI can change the phase and the magnitude of data symbols  $X_n$  for the PAPR reduction purpose while maintaining the system BER. Although TI solves the data rate loss issue of TR, TI increases the system average power in return. In order to alleviate the average power issue, TI applies tone injection on small number of subcarriers only.

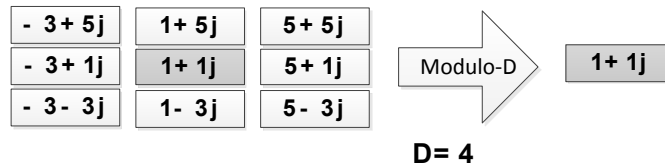


Figure 2.4 An example of 9 different values for mapping the symbol  $1+1j$  in 4-QAM.

Another form of tone injection is the active constellation extension ACE technique (Jones, 1999, Krongold and Jones, 2003). In ACE, only the outer points of constellation diagram are chosen for extension since they have a larger noise margin. In other words, extending the value of the outer points away from its original point will increase its noise margin and enhance BER. Therefore, ACE iterates different selective constellation extension patterns on outer points only and selects the resultant signal with the minimum PAPR. As a result, PAPR is reduced, and average power of transmitted signal is increased.

On the other hand, there are many PAPR reduction techniques that can maintain the average power of the OFDM signal while reducing the PAPR of the transmitted signal. For instance, Interleaving technique iterates  $U$  different permutation patterns to emerge different signals with different PAPR values (Jayalath and Tellambura, 2000a, Jayalath and Tellambura, 2000b, Jayalath and Tellambura, 2001). In other words, interleaving technique shuffle the indices of data symbols according to a predetermined indices permutation mapping sequences known by both transmitter and receiver. Only one resultant signal, with the minimum PAPR, out of  $U$  iterations is selected for transmission. However, in order for the receiver to be able to de-permute the received symbols and recover the original signal, the transmitter needs to send the index of the applied indices permutation mapping sequence to the receiver as

side-information. As a result, some subcarriers are necessarily reserved for side-information.

SLM and PTS, on the other hand, apply phase rotation based scrambling technique for PAPR reduction. In phase rotation based scrambling operation, only the phase is altered for the purpose of PAPR reduction thus the average power is maintained similar as that of the original signal. Phase rotation is achieved by multiplying the symbol  $X_n$  with a complex number of a predetermined phase  $\phi_n^{(u)}$  (i.e.  $X_n e^{j\phi_n^{(u)}}$ ).

In partial transmit sequence (PTS) method presented by (Muller and Huber, 1997b, Müller and Huber, 1997, Cimini and Sollenberger, 1999, 2000), the OFDM data sequence in frequency domain  $X$  is partitioned into  $V$  disjoint sequences of  $N$  length  $X^{(v)}$  so that each symbol  $X_n$  belongs to one partition only. Next, each disjoint sequence  $X^{(v)}$  is converted into time domain signal  $x^{(v)}$  using ifft function. Then, PTS rotates the phase of each partition signal in time domain using a predetermined phase factors  $b_w = e^{j\phi_w} \in B, \phi_w \in [0, 2\pi)$  and sums the rotated partition signals to create the full  $u$ -th OFDM candidate signal. In order to find the optimum combination of phase factors  $\hat{b} = [\hat{b}_1 = 1, \hat{b}_2, \hat{b}_3, \dots, \hat{b}_V], \hat{b}_v \in B$ , PTS will try all possible combination of rotation factors  $W^{V-1}$  where  $W$  denotes the number of allowed phase factors  $b_w$  in  $B = [b_1, b_2, \dots, b_W]$ . It is recommended for implementation flexibility that the first partition is always maintained unrotated so that side-information and pilots placed in are maintained intact. Furthermore, for implementation simplicity, the recommended allowed phase rotation factors are  $\{\pm 1, \pm j\}$  whose phases are  $\{0, \pi, \pm\pi/2\}$  (Müller et al., 1997).

It is worth noting that the partitioning scheme is proven to have great effect on the performance of PAPR reduction in PTS. For instance, the performance of interleaving scheme is better than of adjacent scheme in terms of PAPR reduction. The three possible partitioning schemes for PTS can be seen in Figure 2.5 to Figure 2.7. named adjacent, interleaving, and pseudo-random partitioning schemes.

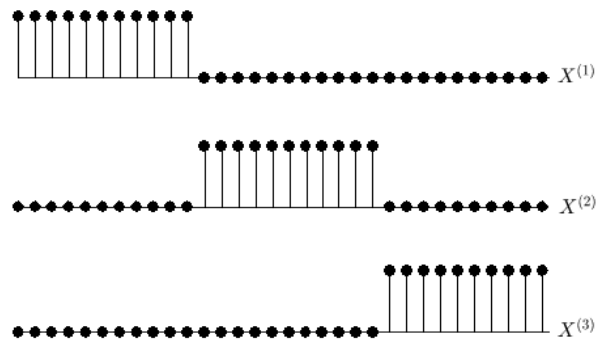


Figure 2.5 An example of dividing subcarriers into 3 disjoint groups using adjacent scheme (Müller et al., 1997).

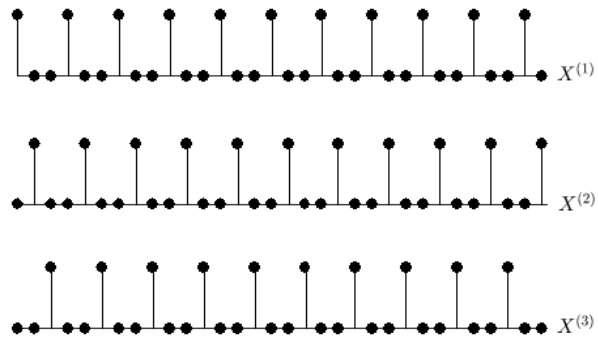


Figure 2.6 An example of dividing subcarriers into 3 disjoint groups using interleaved scheme (Müller and Huber, 1997b).